# *Pseudomonas nanhaiensis* sp. nov., a lipase-producing bacterium isolated from deep-sea sediment of the South China Sea

**Yu Pang**
Biotechnology Research Institute, Chinese Academy of Agricultural Sciences
**Yage Zhang**
Biotechnology Research Institute, Chinese Academy of Agricultural Sciences
**Mengru Chen**
Biotechnology Research Institute, Chinese Academy of Agricultural Sciences
**Wei Lu**
Biotechnology Research Institute, Chinese Academy of Agricultural Sciences
**Ming Chen**
Biotechnology Research Institute, Chinese Academy of Agricultural Sciences
**Yongliang Yan**
Biotechnology Research Institute, Chinese Academy of Agricultural Sciences
**Min Lin**
Biotechnology Research Institute, Chinese Academy of Agricultural Sciences
**Wei Zhang**
Biotechnology Research Institute, Chinese Academy of Agricultural Sciences
**Zhengfu ZHOU** ( zhouzhengfu@caas.cn )
Chinese Academy of Agricultural Sciences Biotechnology Research Institute

**Research Article**

**Keywords:** Pseudomonas nanhaiensis sp. nov., Deep-sea, Sediment, Lipase

**Posted Date:** May 28th, 2021

**DOI:** https://doi.org/10.21203/rs.3.rs-548397/v1



**Version of Record:** A version of this preprint was published at Antonie van Leeuwenhoek on August 14th, 2021. See the published version at https://doi.org/10.1007/s10482-021-01639-y.

## Abstract

A bacterial lipase producer, designated SCS 2–3, was isolated from deep-sea sediment of the South China Sea. Phylogenetic analysis based on the 16S rRNA sequences revealed that strain SCS2-3 belonged to the genus *Pseudomonas* and had 98.56% similarity with *P. xinjiangensis* NRRL B-51270$^T$ that the closest relative strain. MLSA using four protein-coding genes (*dnaK*, *gyrA*, *recA*, and *rpoB*) showed strain SCS 2–3 to branch separately from its most closely related type strains. ANI and in *silico* DDH values between strain SCS 2–3 and the closely related type strains of *Pseudomonas* species were less than 81.51% and 23.80%, respectively, both below the species delineation threshold. Genome comparison showed that strain SCS 2–3 shared 1875 core gene families with other eight closely related type strains in *Pseudomonas*, and the number of strain-unique genes was 263. Through gene annotations, genes related to lipase was found in the isolates' genomes. Furthermore, a combination of phenotypic, chemotaxonomic, phylogenetic and genotypic data clearly indicated that strain SCS 2–3 represents a novel species of the genus *Pseudomonas*, for which the name *Pseudomonas nanhaiensis* sp. nov. is proposed. The type strain is SCS 2-3$^T$ (= GDMCC 1.2219$^T$ = JCM 34440$^T$).


## Introduction

*Pseudomonas* is one of the most studied species of bacteria and is also the genus with the largest number of species(George et al., 2005). The name *Pseudomonas* was first created by professor Migula of the Karlsruhe Institute in Germany at the end of 19th century(Migula, 1895). They are Gram-negative, rod-shaped and polar-flagellated bacteria. The genus *Pseudomonas* belongs to class *Gammaproteobacteria*, order *Pseudomonadales*, family *Pseudomonadaceae* and *Pseudomonas aeruginosa* is described as the type species. At the time of writing, genus *Pseudomonas* includes about 396 species with 21 subspecies (https://lpsn.dsmz.de/search?word=Pseudomonas). *Pseudomonas* species are ubiquitous environmental organisms that occupy several niches, including soils, marine environments, fresh water, plants and animals(Khan et al., 2009; Peix et al., 2009). *Pseudomonas* species are of great interest for biotechnological applications due to the versatile metabolic machinery and their potential for adaptation to fluctuating environmental conditions(Novik et al., 2015). Some of the species have the ability to degrade aromatic compounds(Ma et al., 2012), and others have the important roles in the denitrification process(He et al., 2016). Moreover, some species can promote plant-growth(Ke et al., 2019), whereas others act as pathogens to plants(Oueslati et al., 2019) and animals(Driscoll et al., 2007).

Additionally, *Pseudomonas* is an excellent source of various extracellular enzymes acting as catalysts in specific biochemical reactions(Gilbert, 1993). As a kind of important biocatalysts, *Pseudomonas* lipases are commonly applied in various industrial fields(Gupta et al., 2004). Lipases (EC 3.1.1.3) have been termed triacylglycerol acylhydrolases and are an important group of hydrolases, which catalyze the hydrolysis of natural substrates long-chain triacylglycerols at the lipid-water interface to liberate fatty acids and glycerol(Jaeger et al., 1999). Lipases also have a property to reverse this reaction in an aqueous and non-aqueous media. They play a significant role in a diverse array of biotechnological applications, such as food technology, detergents, waste disposal, biosensor modulations, chemical industry and biomedical sciences(Pandey et al., 1999). Lipases are ubiquitous in nature and are isolated from plants, animals and microorganisms. Microbial lipases, mainly fungal and bacterial origin, are advantageous for industrial applications due to their short generation times, ease of genetic manipulations, scale up and purification(Nagarajan, 2012). Bacterial lipases are generally more used and exhibit higher activity in comparison with fungal lipases(Hasan et al., 2006). Among bacterial lipases, *Pseudomonas* lipases were probably the first to be studied and have an important role in the field of biotechnological applications(Arpigny and JAEGER, 1999).

We therefore screened for lipase-producing bacteria and were able to isolate a bacterial strain SCS 2–3 from deep sea sediment from the South China Sea. Based on phenotypic, chemotaxonomic, phylogenetic, genomic and metabolic characters, we classified strain SCS 2–3 as the genus *Pseudomonas* and strain SCS 2–3 represents a novel species. To reveal the genomic features and the putative ability of lipase production of stain SCS 2–3, we determined its genome sequences and compared its genome with the available genomes of phylogenetically close *Pseudomonas* species.

## Materials And Methods

Sample collection, isolation of bacterial strain and culture conditions

The deep-sea sediment sample was collected from the South China Sea (depth of 1305m, E 117°56.6283', N 20°59.2010'). In detail, 1g sediment sample was enriched in 50ml 2216E liquid medium supplemented with olive oil emulsion for 72h at 28°C, 150 rpm. Then, 200μl of enriched solution was transferred to fresh medium and was cultured at 28°C, 150 rpm for 72h.And this routine was repeated

three times. After, the supernatants of the enriched sample were serially diluted ($10^{-5}$ to $10^{-7}$) with PBS buffer ($KH_2PO_4$ 0.2g, $Na_2HPO_4 \cdot 12H_2O$ 2.9g, NaCl 8g, KCl 0.2g, pH 7.0). 100µl of each diluted sample was spread on 2216E agar plates and incubated at 28°C for 48h. The colonies were aseptically picked and were sub-cultured on Rhodamine B plates(Kouker and Jaeger, 1987) for selecting lipase producing strain.

Phenotypic and biochemical analyses

Colonial and cellular morphology were examined by eye and by scanning electron microscope (SU8010, Hitachi, Japan) and transmission electron microscope (H-7650, Hitachi, Tokyo, Japan). A method for gram-stain reaction determination was modified from Buck's method(Buck, 1982). Growth was observed at various temperatures (4, 15, 20, 25, 28, 30, 33, 37, 40, 45, and 50°C) on 2216E agar medium. Tolerance to different NaCl concentrations (0–10%, in increments of 1%, w/v, NaCl) and pH range (pH 4.0–11.0, at intervals of 1 unit) were performed at 28°C, for 7 days. Anaerobic growth was tested in an MGCAnaeroPouch-Anaero (Mitsubishi, Tokyo, Japan) at 28°C for 7 days on 2216E agar medium. Catalase and oxidase activities were investigated in 3% (v/v) $H_2O_2$ and using commercial strips (Huankai, Guangzhou, China) according to the manufacturer's instruction, respectively. Additional enzyme activities and carbon source utilization assays were examined by using API 20NE, API ZYM (bioMerieux, Marcy-l'Etoile, French) and Biolog plates kits (Hayward, CA, USA), respectively, following the manufacturer's instruction.

Chemotaxonomic analysis

For analysis of the chemotaxonomic features of strain SCS 2–3, a series of experiments were carried out to determine the content of the respiratory quinones, polar lipids, and fatty acids of closely related type strains (*P. xinjiangensis* NRRL B-51270$^T$ and *P. sabulinigri* JCM 14963$^T$) and SCS 2–3. Respiratory quinones of the studied strain were extracted and analyzed via the HPLC system. Polar lipids of strain SCS 2–3 were extracted and examined by two-dimensional TLC. The fatty acids were extracted, quantified, and analyzed using the microbial identification system with strain SCS 2–3 and related type strains.

16S rRNA gene amplification and phylogenetic analysis

Genomic DNA was extracted and purified by a commercial bacterial genomic DNA isolation kit (Magen, Guangzhou, China). PCR amplification of 16S rRNA gene was carried out using bacterial primers F27 and R1492(Weisburg et al., 1991). The amplified fragments were cloned into a cloning-vector pJET1.2/Blunt Vector (Thermo Scientific, Waltham, MA, USA) and sequenced by Sangon Biotech (Shanghai, China). The 16S rRNA gene sequence of strain SCS 2–3 was compared with the EzBioCloud server(Yoon et al., 2017) and closely related type strains with the top 30 of 16S rRNA gene similarity were included in the phylogenetic tree analysis. The phylogenetic tree was constructed using the CLustalW algorithm(Hung and Weng, 2016) from the MEGA version X software package(Kumar et al., 2018) using the neighbor-joining (NJ), maximun likelihood (ML), and maximum parsimonv (MP) methods followed by bootstrap analysis with 1000 bootstrap replications.

MLSA based on housekeeping genes

Multilocus sequence analysis (MLSA) was performed using the method of Maiden et al.(Maiden et al., 1998). The sequences of four protein-coding genes, *dnaK* (1923 bp), *gyrA* (2676 bp), *recA* (1041 bp), and *rpoB* (4068 bp), were obtained from the genome sequences. A phylogenetic tree of concatenated sequences (9708 bp) was reconstructed using the neighbor-joining method. Calculation of distances and multiple alignments and construction of the neighbor-joining phylogenetic tree used the same methods as those of 16S rRNA gene sequences.

The housekeeping genes of closely related type strains with ≥ 97% 16S rRNA sequence similarity with strain SCS 2–3 are available in EzBioCloud database(Yoon et al., 2017). The closed related type strains include *P. xinjiangensis* NRRL B-51270$^T$, *P. sabulinigri* JCM 14963$^T$, *P. populi* KBL-4-9$^T$, *P. gallaeciensis* V113$^T$, *P. pelagia* CL-AP6$^T$, *P. pachastrellae* JCM 12285$^T$, *P. phragmitis* S-6-2$^T$, *P. abyssi* MT5$^T$ and *P. salina* XCD-X85$^T$.

Genome sequencing, de novo assembly and annotation

For genomic DNA extraction and sequencing, strain SCS 2–3 was inoculated from glycerol stocks in TBS liquid medium, and grown for 24h at 28°C, 200 rpm. Then, bacteria were washed in 1×PBS and collected by centrifugation at 5000 rpm for 10 min at 4°C. The

genome of SCS 2–3 was extracted and sequence by Majorbio Bio-pharm Technology Co., Ltd (Shanghai, China) on PacBio and illumina Hiseq ×10 platform. A high-quality data set with a corresponding sequencing depth of 100-fold was generated.

The scan map of the bacterial genome is created using SOAPdenovo2(Luo et al., 2012) and the complete map of the bacterial genome is assembled using canu and SPAdes(Bankevich et al., 2012). Glimmer(Delcher et al., 2007) and GeneMarkS(Besemer and Borodovsky, 2005) were used to predict coding sequences (CDS) and plasmid genes, respectively. tRNA and rRNA were predicted using tRNAscan-SE v2.0(Chan and Lowe, 2019) and Barrnap, respectively. Function annotation of SCS 2–3 was obtained from Non-Redundant Protein (NR), Swiss-Prot(Bairoch and Apweiler, 2000), Pfam(Finn et al., 2014), Clusters of Orthologous Group (COG)(Jensen et al., 2007), Gene Ontology and Kyoto Encyclopedia of Genes(Kanehisa et al., 2016) databases using BLASTp and the same BLAST thresholds. Additionally, the CAZymes were identified, classified and annotated using CAZy database(Lombard et al., 2014).

Comparative genomic analysis

Bacterial Pan Genome Analysis (BPGA), a fast and efficient computational pipeline was used to draw a neighbor-joining phylogenetic tree(Chaudhari et al., 2016). For comparative genomics, the genome sequences of closely related *Pseudomonas* strains were obtained from the EzBioCloud genome database(Yoon et al., 2017) and NCBI genome database. And CDSs of these strains were clustered by USEARCH with identity cut-off at 50%(Edgar, 2010). This analysis utilized all default parameters. The genome average nucleotide identity (ANI) values and digital DNA-DNA hybridization (dDDH) values were calculated using OrthoANI(Lee et al., 2016) and the Genome-to-Genome Distance Calculator (GGDC 2.1)(Meier-Kolthoff et al., 2013), respectively.

Lipase sequence analysis

In our study, ClustalW2 was employed to analyze multiple sequence alignments. Phylogenetic analysis was accomplished using MEGA X with the neighbor-joining method. A bootstrap analysis with 1000 replicates was applied to estimate the reliability of the tree. And visualization was carried out using ESPript 3.1(Robert and Gouet, 2014), which divulge crucial dissimilitude in the lipase as compared to other species. Homology modeling was constructed using the SWISS-MODEL sever(Waterhouse et al., 2018).

## Results And Discussion

Morphological and physiological characteristics

In the present study, strain SCS 2–3 was isolated from deep sea sediment sample from the South China Sea. After 3 days of incubation at 28°C, colonies were yellow, circular and convex with entire edges using tryptic soy broth agar. Cell morphology and size were examined by electron microscopy. SCS 2–3 cells were rod-shaped, measuring approached 0.4μm in width and more than 1.5μm in length on the scanning electron microscope (SEM) and transmission electron microscope (TEM) (Figs. 1A and 1B). Negative-stain transmission electron microscopy showed that cells also contained one polar flagellum (Fig. 1C). Cells of strain SCS 2–3 were Gram-stain-negative and aerobic. The strain SCS 2–3 was capable of growth at temperatures between 10°C and 45°C, and the strain grew well at pH values between 5.0 and 10.0. The strain SCS 2–3 was tolerant to 10% (w/v) NaCl. In addition, strain SCS 2–3 was resistant to Rifamycin SV and Vancomycin. By comparison with two closely related type strains, strain SCS 2–3 differed in a combination of negative oxidase activity and positive glucuronamide metabolism and nitrate reduction (Table 1).

Chemotaxonomic characteristics

The major isoprenoid quinone detected in aerobically grown strain SCS 2–3 was ubiquinone 9, which is consistent with other species in the genus *Pseudomonas*. The polar lipids compositions of strain SCS 2–3 were diphosphatidylglycerol, phosphatidylglycerol, phosphatidylethanolamine and two unknown phospholipids (Supplementary Fig. S1). The cellular fatty acid composition of strain SCS 2–3 and two closely related type strains were characteristics. All strains consisted of the same predominant fatty acids (> 10%) albeit in varying quantities (Supplementary Table S1). The major cellular fatty acids in strain SCS 2–3 were $C_{18:1}$ $\omega 6c/\omega 7c$, $C_{16:1}$ $\omega 6c/_{16:1}$ $\omega 7c$, and $C_{16:0}$. Strain SCS 2–3 also has unique fatty acid anteiso $C_{17:1}\omega 9c$ which was not detected in other 2 close relatives. The different fatty acid profile is also an evidence to distinguish strain SCS 2–3 from others in *Pseudomonas*.

Phylogenetic characteristics

The complete 16S rRNA gene sequence (1532 bp) of strain SCS 2–3 was compared with other type strains with the top 30 of sequence similarity using phylogenetic tree analysis. On the basis of 16S rRNA gene sequence homology, the closest relatives were determined to

be *P. xinjiangensis* NRRL B-51270$^T$ (98.56%), *P. sabulinigri* JCM 14963$^T$ (97.94%), *P. populi* KBL-4-9$^T$ (97.67%), *P. gallaeciensis* V113$^T$ (97.29%), *P. pelagia* CL-AP6$^T$ (97.26%), *P. pachastrellae* JCM 12285$^T$ (97.19%), *P. phragmitis* S-6-2$^T$ (97.19%), *P. abyssi* MT5$^T$ (97.15%) and *P. salina* XCD-X85$^T$ (97.12%). The NJ phylogenetic tree revealed that strain SCS 2–3 clustered with members of the genus *Pseudomonas* and formed a monophyletic clade with *P. xinjiangensis* NRRL B-51270$^T$ (Fig. 2).

To further confirm the phylogenetic position of strain SCS 2–3, we performed MLSA based on four protein-coding fragments of the *dnaK*, *gyrA*, *recA*, and *rpoB* gene sequence (Supplementary Fig. S2). The sequence similarities between strain SCS 2–3 and related *Pseudomonas* type strain are summarized in Table 2. The most closely related *Pseudomonas* type strain was *P. xinjiangensis* NRRL B-51270$^T$ with 88.3% sequence similarity, and the strain SCS 2–3 formed a clear branch away from that stain (Supplementary Fig. S2).

Genomic characteristics

The complete genome sequence of strain SCS 2–3 was assembled into a ring chromosome with 3,653,147bp (Fig. 3). The DNA G + C content of strain SCS 2–3 was 61.22%, which is a value within the range (58–71%) for the genus *Pseudomonas* and nearly equal to that of *P. xinjiangensis* NRRL B-51270$^T$, the closest phylogenetic relative which is 60.7%. SCS 2–3 contained 51 tRNAs and 9 rRNAs (Table 3). A length of 3,287,676bp genes was found based on gene prediction, and the ratio of gene length/genome was 90.00%. The intergene region/genome ratio was 10.00%, and the GC contents of the gene and intergene region were 61.70% and 56.89%, respectively.

Furthermore, 3379 CDSs were contained in the genome, and the average length of gene was 972.97bp. CDSs were further annotated in NR, Swiss-Port, Pfm, COG, kEGG, GO and CAZy databases, and their numbers were 3379, 2566, 2940, 3049, 2288, 1977 and 93, respectively.

Comparison with closely related bacterial strains

The genome of strain SCS 2–3 was compared to the available genome of eight closely related bacterial Type strains. This comparison revealed that the genome size of our strain (3.65Mb) was larger than that of *P. xinjiangensis* NRRL B-51270$^T$ (3.54Mb), but smaller than those of *P. sabulinigri* JCM 14963$^T$, *P. gallaeciensis* V113$^T$, *P. pelagia* CL-AP6$^T$, *P. pachastrellae* JCM 12285$^T$, *P. phragmitis* S-6-2$^T$, *P. abyssi* MT5$^T$, and *P. salina* XCD-X85$^T$ (4.03, 4.25, 4.64, 3.93, 4.04, 4.32 and 4.26Mb, respectively) (Table 3). The G + C content of strain SCS 2–3 (61.22%) was equal to that of *P. xinjiangensis* NRRL B-51270$^T$, *P. gallaeciensis* V113$^T$, *P. pachastrellae* JCM 12285$^T$, and *P. abyssi* MT5$^T$, but greater than the other compare species (Table 3). The CDSs of strain SCS 2–3 (3379) was similar to that of *P. xinjiangensis* NRRL B-51270$^T$, but smaller than those of the others. The distribution of genes into COG categories was similar in all nine compares genomes (Supplementary Fig. S3). A total 9 genomes were analyzed for comparison with BPGA. The analysis was carried out based on all translated protein sequence comparison. It seems that *Pseudomonas* species have open pan-genome, suggesting that continuous new genes are being added to the pangenome and hence, with the addition of new genome, leads to an increase in accessory and unique genes number and decrease in core genes number (Supplementary Fig. S4). To measure phylogenetic relationships, the CDSs of each strain were used for phylogenetic analysis. The core genome sequences of individual strain were calculated. The resulting phylogenetic analysis indicated that strain SCS 2–3 formed a monophyletic clade with *P. xinjiangensis* NRRL B-51270$^T$ (Supplementary Fig. S5). Moreover, 1857 (10.55%) shared orthologous coding sequences were clustered into the core genome of 9 strains, 11,946 (67.87%) were represented in the accessory genome, and 3798 (21.58%) were identified as strain-unique genes (Supplementary Fig. S5). Fonctional COG annotation revealed that the core genome had a higher proportion of genes classified in COG categories J (translation, ribosomal structure, and biogenesis), E (Amino acid transport and metabolism), H (Coenzyme transport and metabolism), and O (Posttranslational modification, protein turnover, chaperones), all associated with basic biological functions. The accessory genome and strain-specific genes were biased toward COG categories T (Signal transduction mechanisms), V (Defense mechanisms), K (Transcription) and P (Inorganic ion transport and metabolism) (Supplementary Fig. S6), which were probably related to the adaption of *Pseudomonas* to various kinds of environments.

DNA-DNA hybridization is required for discrimination of microbial species in cases where 16S rRNA gene sequence similarities are 97% or higher(Spencer et al., 1984). To determine the taxonomic characteristics of strain SCS 2–3, digital DNA-DNA relatedness between strain SCS 2–3 and its related Pseudomonas type strains was conducted. The analysis revealed that strain SCS 2–3 had fairly low levels of DNA-DNA relatedness to *P. xinjiangensis* NRRL B-51270$^T$ (23.80%), *P. sabulinigri* JCM 14963$^T$ (19.50%), *P. gallaeciensis* V113$^T$ (19.70%), *P. pelagia* CL-AP6$^T$ (19.50%), *P. pachastrellae* JCM 12285$^T$ (19.80%), *P. phragmitis* S-6-2$^T$ (19.60%), *P. abyssi* MT5$^T$ (19.90%)

and *P. salina* XCD-X85$^T$ (18.90%) (Table 2). The ANI between genome sequences of strain SCS 2–3 and closely related type strains (16S rRNA gene similarity ≥ 97%) varied between 73.79–81.51% (Table 2). The ANI values are lower than the 95% threshold value(Thompson et al., 2013) and the dDDH values are significantly lower than the 70% threshold value(Wayne et al., 1987). Thus, based on the presented phenotypic and genomic data, we propose the creation of *Pseudomonas sp*. nov., as a new species belonging to the *Pseudomonas* genus with strain SCS 2–3 as its type strain.

KEGG annotations

KEGG function-based classification and metabolic pathway analysis was used to identify metabolism pathways of strain SCS 2–3. As shown in Supplementary Fig. S7, of the six classification of KEGG pathway, this analysis revealed 39 functional groups. Metabolism contained the most numbers of genes, followed by environmental information processing. In KEGG metabolism annotations of strain SCS 2–3, amino acid metabolism and carbohydrate metabolism which are considered its main functions, contained 191 and 162 genes, respectively (Supplementary Fig. S7). For these metabolisms, there were some dominant pathways, such as pyruvate metabolism (ko00620) and glyoxylate and dicarboxylate metabolism (ko00630). Forty-one genes were related to ko00620, and the important regulatory enzyme pyruvate kinase (EC:2.7.1.40), present in ko00620, was involved in glycolysis. In ko00630, 39 genes were found, in which malate was oxidized into oxaloacetate. In addition, ko00630 was linked with other pathways. For instance, oxaloacetate was condensed into citrate, which has an ability to enter the citrate cycle.

The annotation involved in the lipid metabolism has also been identified. For lipid metabolism, it contained 69 genes. Fatty acid degradation (ko00071), fatty acid biosynthesis (ko00061) and glycerophospholipid metabolism (ko00564) were dominant pathways. Twenty-four genes were related to ko00071, and acyl-CoA dehydrogenase (EC:1.3.8.7) and long-chain acyl-CoA synthetase (EC:6.2.1.3), present in ko00071, were involved in Fatty acid β-oxidation. In the genome, 22 genes were found in ko00061 and 18 genes were found in ko00564. Also, glycerolipid metabolism (ko00561) was 10 genes including triacylglycerol lipase (EC:3.1.1.3) which hydrolyses triglycerides into diglycerides and subsequently into monoglycerides and free fatty acids.

lipase-producing capability and lipase sequence analysis for strain SCS 2–3

To identify the strain SCS 2–3 as lipase producers, it was incubated on rhodamine B agar plates for 72h at 28°C. Then the plate was subjected to UV irradiation (365 nm) and photographed (Supplementary Fig. S9). As shown in the result, strain SCS 2–3 formed an orange fluorescent zone around the strain on a UV trans illuminator and had the lipase activity.

In general, lipases from *Pseudomonas* have be classified into three categories, and they all belong to family I(Rosenau and Jaeger, 2000). Family I.1 lipases have molecular massed in the range 30–32 kDa and display a higher sequence similarity to the *Pseudomonas aeruginosa* lipase. The crystal structure of the *Pseudomonas aeruginosa* lipase was solved(Nardini et al., 2000) providing the first structure in the lipases of Family I.1. Lipases from family I.2 are characterized by a slightly larger size (33 kDa) owing to an insertion in the amino acid sequence forming an anti-parallel double β-strand at the surface of the molecule(Noble et al., 1993; Kim et al., 1997). The expression in an active form of lipases belonging to family I.1 and I.2 depends on a molecular chaperone named lipase-specific foldase (Lif) and these lipases provide classic signal peptide to secretion through cell membrane. Lipases from family I.3 have in common a higher molecular mass than lipases from family I.1 and I.2 and the absence of an N-terminal signal peptide and of Cys residues. The secretion of these lipases occurs through a three-component ATP-bind-cassette transporter system(Rosenau and Jaeger, 2000; Zhao et al., 2007). There are 9 genes of *Pseudomonas* lipases reviewed in UniprotKB database(Consortium, 2019) (Supplementary Table S2).

The strain SCS 2–3 has lipase activity. In the results of its genome annotation, one lipase gene (Gene ID: gene0160) was found. The lipase gene encoded a 311 amino acid sequence with a theoretical molecular mass of 32.86 kDa. According to the identity of the amino acid sequence, this lipase gene sequence was compared with the above reference sequences, and the NJ phylogenetic tree was constructed from the comparison results (Fig. 4A). As shown in Fig. 4A, the lipase of strain SCS 2–3 belongs to family I.1.

The family I.1 lipases was investigated to scrutinize the relatedness (Fig. 4B); subsequently, less variations were detected and the major portion of the protein remain conserved among the species under investigation. The observed sequence variations in Lipases have been highlighted in white columns and the conserved one in red (Fig. 4B).

Three-dimensional protein structure provides valuable insights into the molecular basis of protein function. Using *in silico* techniques the structure and potential function of the lipase was elucidated. The structural protein sequence of the lipase is shown in Fig. 4B. The

FASTA sequence of the lipase was entered into the SWISS-MODEL server. Based on the sequence, the structure of the molecule was predicted (Fig. 4C). The most appropriate template for homology modeling is the crystal structure of the lipase (Accession No. 1ex9.1.A ) from *P. aeruginosa*. The identity of amino acid sequence was 82.69% between lipase and 1ex9.1.A. The 3D structure showed a variant of the α/β hydrolase fold, and the Ser108, Asp255 and His277 as the catalytic active center (Figs. 4B and 4C).

## Conclusion

Marine sediments harbor an extraordinary range of various and complex microbial communities(Lozupone and Knight, 2005). Here we aimed at describing a novel bacterial species to enrich the knowledge on the Marine microbial communities. The phylogenetic and phenotypic analysis of the new strain SCS 2–3 exhibited several distinct traits compared to other strains of the genus *Pseudomonas*. Hence strain SCS 2–3 is a novel species of the genus *Pseudomonas* for which the name *Pseudomonas nanhaiensis* sp. nov. is suggested, its protologue description is list in Table 4. Furthermore, strain SCS 2–3 showed lipolytic activity using rhodamine B agar plates and a novel lipase from strain SCS 2–3 was discovered in this study.

## Declarations

# Author contribution

Z.Z. and W.Z. designed research and project outline. Y.P., Y.Z., M.C., and M.C. performed isolation, deposition and polyphasic taxonomy. Y. P. and Y.Y. performed genome analysis. W.L.and W. Z. contributed to the polar lipid analysis. Y.P. and Z.Z.drafted the manuscript. M.L. revised the manuscript. All authors read and approved the final manuscript.

# Funding

This work was supported by National Key R&D Program of China (No.2018YFA0901000□2018YFA0901003), the National Transgenic Major Program of China (No. 2019ZX08010-004), the National Natural Science Foundation of China (No. 31930004). We also appreciate the support of the Agricultural Science and Technology Innovation Program of CAAS (No. CAAS-ZDRW202009).

# Conflict of Interest

The authors declare that there are no conflicts of interest.

# Ethical approval

This article does not contain any studies with human participants or animals performed by any of the authors.

## References

Arpigny, J.L., and JAEGER, K.-E. (1999). Bacterial lipolytic enzymes: classification and properties. Biochem. J. 343, 177-183.

Bairoch, A., and Apweiler, R. (2000). The SWISS-PROT protein sequence database and its supplement TrEMBL in 2000. Nucleic Acids Res. 28, 45-48.

Bankevich, A., Nurk, S., Antipov, D., Gurevich, A.A., Dvorkin, M., Kulikov, A.S., Lesin, V.M., Nikolenko, S.I., Pham, S., and Prjibelski, A.D. (2012). SPAdes: a new genome assembly algorithm and its applications to single-cell sequencing. J. Comput. Biol. 19, 455-477.

Besemer, J., and Borodovsky, M. (2005). GeneMark: web software for gene finding in prokaryotes, eukaryotes and viruses. Nucleic Acids Res. 33, W451-W454.

Buck, J.D. (1982). Nonstaining (KOH) method for determination of gram reactions of marine bacteria. Appl. Environ. Microbiol. 44, 992-993.

Chan, P.P., and Lowe, T.M. (2019) tRNAscan-SE: searching for tRNA genes in genomic sequences. In Gene Prediction. Springer, pp. 1-14.

Chaudhari, N.M., Gupta, V.K., and Dutta, C. (2016). BPGA-an ultra-fast pan-genome analysis pipeline. Sci. Rep. 6, 1-10.

Consortium, U. (2019). UniProt: a worldwide hub of protein knowledge. Nucleic Acids Res. 47, D506-D515.

Delcher, A.L., Bratke, K.A., Powers, E.C., and Salzberg, S.L. (2007). Identifying bacterial genes and endosymbiont DNA with Glimmer. Bioinformatics 23, 673-679.

Driscoll, J.A., Brody, S.L., and Kollef, M.H. (2007). The epidemiology, pathogenesis and treatment of Pseudomonas aeruginosa infections. Drugs 67, 351-368.

Edgar, R.C. (2010). Search and clustering orders of magnitude faster than BLAST. Bioinformatics 26, 2460-2461.

Finn, R.D., Bateman, A., Clements, J., Coggill, P., Eberhardt, R.Y., Eddy, S.R., Heger, A., Hetherington, K., Holm, L., and Mistry, J. 2014. Pfam: the protein families database. *Nucleic Acids Res.* 42, D222-D230.

George, M., Julia, A., and Timothy, G. (2005) Bergey's Manual of Systematic Bacteriology 2nded Vol. 2. New York: Springer.

Gilbert, E.J. (1993). Pseudomonas lipases: biochemical properties and molecular cloning. Enzyme Microb. Technol. 15, 634-645.

Gupta, R., Gupta, N., and Rathi, P. (2004). Bacterial lipases: an overview of production, purification and biochemical properties. Appl. Microbiol. Biotechnol. 64, 763-781.

Hasan, F., Shah, A.A., and Hameed, A. (2006). Industrial applications of microbial lipases. Enzyme Microb. Technol. 39, 235-251.

He, T., Li, Z., Sun, Q., Xu, Y., and Ye, Q. (2016). Heterotrophic nitrification and aerobic denitrification by Pseudomonas tolaasii Y-11 without nitrite accumulation during nitrogen conversion. Bioresour. Technol. 200, 493-499.

Hung, J.-H., and Weng, Z. (2016). Sequence alignment and homology search with BLAST and ClustalW. Cold Spring Harb. *Protoc.* 2016, pdb. prot093088.

Hwang, C.Y., Zhang, G.I., Kang, S.-H., Kim, H.J., and Cho, B.C. (2009). Pseudomonas pelagia sp. nov., isolated from a culture of the Antarctic green alga Pyramimonas gelidicola. Int J Syst Evol Microbiol 59, 3019-3024.

Jaeger, K., Dijkstra, B., and Reetz, M. (1999). Bacterial biocatalysts: molecular biology, three-dimensional structures, and biotechnological applications of lipases. Annu. Rev. Microbiol. 53, 315-351.

Jensen, L.J., Julien, P., Kuhn, M., von Mering, C., Muller, J., Doerks, T., and Bork, P. (2007). eggNOG: automated construction and annotation of orthologous groups of genes. Nucleic Acids Res. 36, D250-D254.

Kanehisa, M., Sato, Y., Kawashima, M., Furumichi, M., and Tanabe, M. (2016). KEGG as a reference resource for gene and protein annotation. Nucleic Acids Res. 44, D457-D462.

Ke, X., Feng, S., Wang, J., Lu, W., Zhang, W., Chen, M., and Lin, M. (2019). Effect of inoculation with nitrogen-fixing bacterium Pseudomonas stutzeri A1501 on maize plant growth and the microbiome indigenous to the rhizosphere. Syst. Appl. Microbiol. 42, 248-260.

Khan, N.H., Ahsan, M., Taylor, W.D., and Kogure, K. (2009). Culturability and survival of marine, freshwater and clinical Pseudomonas aeruginosa. Microbes Environ., 1008090221-1008090221.

Kim, K.-H., Roh, S.W., Chang, H.-W., Nam, Y.-D., Yoon, J.-H., Jeon, C.O., Oh, H.-M., and Bae, J.-W. (2009). Pseudomonas sabulinigri sp. nov., isolated from black beach sand. Int J Syst Evol Microbiol 59, 38-41.

Kim, K.K., Song, H.K., Shin, D.H., Hwang, K.Y., and Suh, S.W. (1997). The crystal structure of a triacylglycerol lipase from Pseudomonas cepacia reveals a highly open conformation in the absence of a bound inhibitor. Structure 5, 173-185.

Kouker, G., and Jaeger, K.-E. (1987). Specific and sensitive plate assay for bacterial lipases. Appl. Environ. Microbiol. 53, 211-213.

Kumar, S., Stecher, G., Li, M., Knyaz, C., and Tamura, K. (2018). MEGA X: molecular evolutionary genetics analysis across computing platforms. Mol. Biol. Evol. 35, 1547-1549.

Lee, I., Kim, Y.O., Park, S.-C., and Chun, J. (2016). OrthoANI: an improved algorithm and software for calculating average nucleotide identity. Int J Syst Evol Microbiol 66, 1100-1103.

Li, J., Wang, L.-h., Xiang, F.-g., Ding, W.-l., Xi, L.-j., Wang, M.-q., Xiao, Z.-j., and Liu, J.-g. (2020). Pseudomonas phragmitis sp. nov., isolated from petroleum polluted river sediment. Int J Syst Evol Microbiol 70, 364-372.

Liu, M., Luo, X., Zhang, L., Dai, J., Wang, Y., Tang, Y., Li, J., Sun, T., and Fang, C. (2009). Pseudomonas xinjiangensis sp. nov., a moderately thermotolerant bacterium isolated from desert sand. Int J Syst Evol Microbiol 59, 1286-1289.

Lombard, V., Golaconda Ramulu, H., Drula, E., Coutinho, P.M., and Henrissat, B. (2014). The carbohydrate-active enzymes database (CAZy) in 2013. Nucleic Acids Res. 42, D490-D495.

Lozupone, C., and Knight, R. (2005). UniFrac: a new phylogenetic method for comparing microbial communities. Appl. Environ. Microbiol. 71, 8228-8235.

Luo, R., Liu, B., Xie, Y., Li, Z., Huang, W., Yuan, J., He, G., Chen, Y., Pan, Q., and Liu, Y. (2012). SOAPdenovo2: an empirically improved memory-efficient short-read de novo assembler. GigaScience 1, 2047-2217X-2041-2018.

Ma, J., Xu, L., and Jia, L. (2012). Degradation of polycyclic aromatic hydrocarbons by Pseudomonas sp. JM2 isolated from active sewage sludge of chemical plant. J Environ Sci (China) 24, 2141-2148.

Maiden, M.C., Bygraves, J.A., Feil, E., Morelli, G., Russell, J.E., Urwin, R., Zhang, Q., Zhou, J., Zurth, K., and Caugant, D.A. (1998). Multilocus sequence typing: a portable approach to the identification of clones within populations of pathogenic microorganisms. PNAS 95, 3140-3145.

Meier-Kolthoff, J.P., Auch, A.F., Klenk, H.-P., and Göker, M. (2013). Genome sequence-based species delimitation with confidence intervals and improved distance functions. BMC Bioinform. 14, 1-14.

Migula, W. (1895) *Über ein neues System der Bakterien*.

Mulet, M., Sánchez, D., Rodríguez, A.C., Nogales, B., Bosch, R., Busquets, A., Gomila, M., Lalucat, J., and García-Valdés, E. (2018). Pseudomonas gallaeciensis sp. nov., isolated from crude-oil-contaminated intertidal sand samples after the Prestige oil spill. Syst. Appl. Microbiol. 41, 340-347.

Nagarajan, S. (2012). New tools for exploring “old friends—microbial lipases”. Appl. Biochem. Biotechnol. 168, 1163-1196.

Nardini, M., Lang, D.A., Liebeton, K., Jaeger, K.-E., and Dijkstra, B.W. (2000). Crystal structure of Pseudomonas aeruginosa lipase in the open conformation: the prototype for family I. 1 of bacterial lipases. J. Biol. Chem. 275, 31219-31225.

Noble, M., Cleasby, A., Johnson, L., Egmond, M., and Frenken, L. (1993). The crystal structure of triacylglycerol lipase from Pseudomonas glumae reveals a partially redundant catalytic aspartate. FEBS Lett. 331, 123-128.

Novik, G., Savich, V., and Kiseleva, E. (2015). An insight into beneficial Pseudomonas bacteria. Microbiology in agriculture and human health, 73-105.

Oueslati, M., Mulet, M., Gomila, M., Berge, O., Hajlaoui, M.R., Lalucat, J., Sadfi-Zouaoui, N., and García-Valdés, E. (2019). New species of pathogenic Pseudomonas isolated from citrus in Tunisia: Proposal of Pseudomonas kairouanensis sp. nov. and Pseudomonas nabeulensis sp. nov. Syst. Appl. Microbiol. 42, 348-359.

Pandey, A., Benjamin, S., Soccol, C.R., Nigam, P., Krieger, N., and Soccol, V.T. (1999). The realm of microbial lipases in biotechnology. Biotechnol. Appl. Biochem. 29, 119-131.

Peix, A., Ramírez-Bahena, M.-H., and Velázquez, E. (2009). Historical evolution and current status of the taxonomy of genus Pseudomonas. *I*nfect. Genet. Evol. 9, 1132-1147.

Robert, X., and Gouet, P. (2014). Deciphering key features in protein structures with the new ENDscript server. Nucleic Acids Res. 42, W320-W324.

Romanenko, L.A., Uchino, M., Falsen, E., Frolova, G.M., Zhukova, N.V., and Mikhailov, V.V. (2005). Pseudomonas pachastrellae sp. nov., isolated from a marine sponge. Int J Syst Evol Microbiol 55, 919-924.

Rosenau, F., and Jaeger, K.-E. (2000). Bacterial lipases from Pseudomonas: regulation of gene expression and mechanisms of secretion. Biochimie 82, 1023-1032.

Spencer, D.F., Schnare, M.N., and Gray, M.W. (1984). Pronounced structural similarities between the small subunit ribosomal RNA genes of wheat mitochondria and Escherichia coli. PNAS 81, 493-497.

Thompson, C.C., Chimetto, L., Edwards, R.A., Swings, J., Stackebrandt, E., and Thompson, F.L. (2013). Microbial genomic taxonomy. BMC Genom. 14, 1-8.

Waterhouse, A., Bertoni, M., Bienert, S., Studer, G., Tauriello, G., Gumienny, R., Heer, F.T., de Beer, T.A.P., Rempfer, C., and Bordoli, L. (2018). SWISS-MODEL: homology modelling of protein structures and complexes. Nucleic Acids Res. 46, W296-W303.

Wayne, L., Brenner, D., Colwell, R., Grimont, P., Kandler, O., Krichevsky, M., Moore, L., Moore, W., Murray, R., and Stackebrandt, E. (1987). Report of the ad hoc committee on reconciliation of approaches to bacterial systematics. Int J Syst Evol Microbiol 37, 463-464.

Wei, Y., Mao, H., Xu, Y., Zou, W., Fang, J., and Blom, J. (2018). Pseudomonas abyssi sp. nov., isolated from the abyssopelagic water of the Mariana Trench. Int J Syst Evol Microbiol 68, 2462-2467.

Weisburg, W.G., Barns, S.M., Pelletier, D.A., and Lane, D.J. (1991). 16S ribosomal DNA amplification for phylogenetic study. J. Bacteriol. 173, 697-703.

Yoon, S.-H., Ha, S.-M., Kwon, S., Lim, J., Kim, Y., Seo, H., and Chun, J. (2017). Introducing EzBioCloud: a taxonomically united database of 16S rRNA gene sequences and whole-genome assemblies. Int J Syst Evol Microbiol 67, 1613.

Zhao, X., El-Zahab, B., Brosnahan, R., Perry, J., and Wang, P. (2007). An organic soluble lipase for water-free synthesis of biodiesel. Appl. Biochem. Biotechnol. 143, 236-243.

Zhong, Z.-P., Liu, Y., Hou, T.-T., Liu, H.-C., Zhou, Y.-G., Wang, F., and Liu, Z.-P. (2015). Pseudomonas salina sp. nov., isolated from a salt lake. Int J Syst Evol Microbiol 65, 2846-2851.

# Tables

**Table 1** Differential physiological characteristics between strain SCS 2-3 and closely related type strains.

All data are from this study.

Strains: 1, SCS 2-3; 2, *P. xinjiangensis* NRRL B-51270$^{T}$; 3, *P. sabulinigri* JCM 14963$^{T}$.

+: positive; w: weakly positive; -: negative.

| characteristic | 1 | 2 | 3 |
|---|---|---|---|
| Production of Catalase | + | + | + |
| Oxidase | - | + | + |
| Nitrate reductase | + | - | - |
| Tween 80 hydrilysis | + | + | + |
| Alkaline phosphatase | + | w | w |
| Esterase (C4) | + | + | + |
| Lipid esterase (C8) | + | + | + |
| Lipid enzyme (C14) | + | - | + |
| Leucine arylamidase | + | + | + |
| Trypsin | w | w | - |
| Acid phosphatase | w | w | + |
| Utilization of | | | |
| Dextrin | - | - | w |
| D-Fructose | - | w | - |
| D-Fucose | - | w | - |
| L-Fucose | - | w | - |
| L-Rhamnose | - | - | w |
| 1% Sodium lactate | - | - | + |
| Fusidic acid | - | w | + |
| D-Fructose-6-PO4 | w | w | w |
| Troleand omycin | - | w | - |
| Rifamycin SV | w | + | + |
| L-Alanine | - | + | + |
| L-Glutamic acid | - | - | + |
| L-Pyroglutamic acid | - | - | w |
| Lincomycin | - | w | w |
| D-Galacturonic acid | w | w | - |
| L-Galactonic acid lactone | - | w | - |
| Glucuronamide | + | w | w |
| Vancomycin | w | + | w |
| Methyl pyruvate | - | + | + |
| D-Lactic acid methyl ester | - | - | W |
| L-Lactic acid | - | - | + |
| Citric acid | - | - | + |
| α-keto-glutaric acid | - | - | w |
| D-Malic acid | - | - | w |

| | | | |
|---|---|---|---|
| Potassium tellyrite | - | w | - |
| Tween 40 | - | + | + |
| β-hydroxy-D, L butyric acid | - | w | + |
| Acetoacetic acid | - | w | + |
| Propionic acid | - | w | + |
| Acetic acid | - | + | + |
| Aztreonam | - | + | - |
| Sodium butyrate | - | w | - |

**Table 2** Sequence similarity, ANI and dDDH of strain SCS 2-3 and the related type strains in genus *Pseudomonas*.

| Strains | Strain SCS 2-3 (%) | | | | | | ANI | dDDH |
|---|---|---|---|---|---|---|---|---|
| | 16S rRNA | *dnaK* | *gyrA* | *recA* | *rpoB* | MLSA | | |
| *P. xinjiangensis* NRRL B-51270$^T$ | 98.56 | 87.7 | 87.3 | 86.1 | 89.9 | 88.3 | 81.51 | 23.80 |
| *P. sabulinigri* JCM 14963$^T$ | 97.94 | 85.7 | 75.9 | 84.8 | 87.1 | 83.4 | 74.59 | 19.50 |
| *P. gallaeciensis* V113$^T$ | 97.29 | 84.1 | 78.2 | 85.4 | 86.9 | 83.6 | 74.56 | 19.70 |
| *P. pelagia* CL-AP6$^T$ | 97.26 | 83.6 | 76.3 | 86.3 | 85.4 | 82.5 | 74.23 | 19.50 |
| *P. pachastrellae* JCM 12285$^T$ | 97.19 | 84.6 | 77.2 | 85.3 | 87.0 | 83.4 | 74.68 | 19.80 |
| *P. phragmitis* S-6-2$^T$ | 97.19 | 85.4 | 75.4 | 85.1 | 86.6 | 83.0 | 75.43 | 19.60 |
| *P. abyssi* MT5$^T$ | 97.15 | 84.2 | 78.3 | 85.0 | 86.7 | 83.5 | 74.48 | 19.90 |
| *P. salina* XCD-X85$^T$ | 97.12 | 84.6 | 75.9 | 83.9 | 85.8 | 82.5 | 73.79 | 18.90 |

**Table 3** General features of the analyzed genomes of *Pseudomonas* strains

| Genome | GenBank assembly no. | Isolation origin | No. of contigs | Total bases | No. of CDSs | No. of rRNAs | No. of tRNAs | GC content | Ref. |
|---|---|---|---|---|---|---|---|---|---|
| *Pseudomonas nanhaiensis* SCS 2-3 | CP073751 | deep sea sediment | 1 | 3,653,147 | 3,379 | 9 | 51 | 61.2% | |
| *P. xinjiangensis* NRRL B-51270$^T$ | LT629736 | desert sand | 1 | 3,537,092 | 3,280 | 9 | 50 | 60.7% | (Liu *et al.*, 2009) |
| *P. sabulinigri* JCM 14963$^T$ | LT629763 | black sand | 1 | 4,030,203 | 3,637 | 9 | 51 | 59.9% | (Kim *et al.*, 2009) |
| *P. gallaeciensis* V113$^T$ | FN995250 | crude-oil-contaminated intertidal sand sample | 18 | 4,246,542 | 3,919 | 3 | 46 | 61.5% | (Mulet *et al.*, 2018) |
| *P. pelagia* CL-AP6$^T$ | AROI01000066 | culture of Pyramimonas gelidicola established from the Antarctic | 81 | 4,642,307 | 4,261 | 3 | 46 | 57.4% | (Hwang *et al.*, 2009) |
| *P. pachastrellae* JCM 12285$^T$ | MUBC01000081 | marine sponge | 55 | 3,934,694 | 3,663 | 8 | 49 | 61.2% | (Romanenko *et al.*, 2005) |
| *P. phragmitis* S-6-2$^T$ | CP020100 | petroleum polluted river(Host: sediment) | 1 | 4,035,153 | 3,703 | 9 | 51 | 60.1% | (Li *et al.*, 2020) |
| *P. abyssi* MT5$^T$ | MF962536 | Deep Sea Water | 79 | 4,322,744 | 3,999 | 4 | 46 | 61.2% | (Wei *et al.*, 2018) |
| *P. salina* XCD-X85$^T$ | KC762324 | Salt lake | 45 | 4,256,268 | 3,858 | 10 | 49 | 57.5% | (Zhong *et al.*, 2015) |

**Table 4** rotologue description of *Pseudomonas nanhaiensis* sp. nov.

| | |
|---|---|
| **Genus name** | *Pseudomonas* |
| **Species name** | *Pseudomonas nanhaiensis* |
| **Specific epithet** | *nanhaiensis* |
| **Species status** | sp. nov. |
| **Species etymology** | nan.hai.en'sis. N.L. fem. adj. nanhaiensis pertaining to Nanhai, a sea in South China where the sample was isolated |
| **Description of the new taxon and diagnostic traits** | Cells are Gram-stain-negative, aerobic, motile, rods, catalase positive, oxidase negative, and have a diameter varying from 0.4μm to 0.6μm. The colonies are yellow, circular and convex with entire edges on tryptic soy broth agar. Growth occurs at temperatures in the range 10-45°C. Cells can grow in a range of pH from 5.0-12.0. Cells can grow without NaCl but also be tolerant to 10% (w/v) NaCl. Cells can reduce nitrate to nitrite. Positive for hydrolysis of Tween 80, and negative for amylum, casein, gelatin and urea. This strain has a positive reaction was observed for alkaline phosphatase, esterase (C4), lipase esterase (C8), lipid enzyme (C14) and leucine arylamidase. It is able to utilize D-fructose-6-$PO_4$, D-galacturonic acid, D-glucuronic acid and glucuronamide as carbon sources for growth. The major fatty acids of strain SCS 2-3 are $C_{18:1}$ *ω6c/ω7c*, $C_{16:1}$ *ω6c/*$_{16:1}$ *ω7c*, and $C_{16:0}$. The predominant isoprenoid quinone detected in aerobically grown cells of strain SCS 2-3 is ubiquinone 9. The polar lipids compositions of strain SCS 2-3 were diphosphatidylglycerol, phosphatidylglycerol, phosphatidylethanolamine and two unknown phospholipids. |
| **country of origin** | China |
| **Region of origin** | the South China Sea |
| **Source of isolation** | deep-sea sediment |
| **Sampling date** | 08/11/2018 |
| **Latitude** | 20°59.2010'N |
| **Longitude** | 117°56.6283'E |
| **16S rRNA gene accession nr.** | MZ027638 |
| **Genome accession number** | GenBank = CP073751 |
| **Genome status** | complete |
| **Genome size** | 3653 kbp |
| **GC mol%** | 61.22 |
| **Number of strains in study** | 1 |
| **Information related to the Nagoya Protocol** | Not applicable |
| **Designation of the type strain** | SCS 2-3$^T$ |
| **Strain collection** | GDMCC 1.2219$^T$= JCM 34440$^T$ |

numbers

## Figures

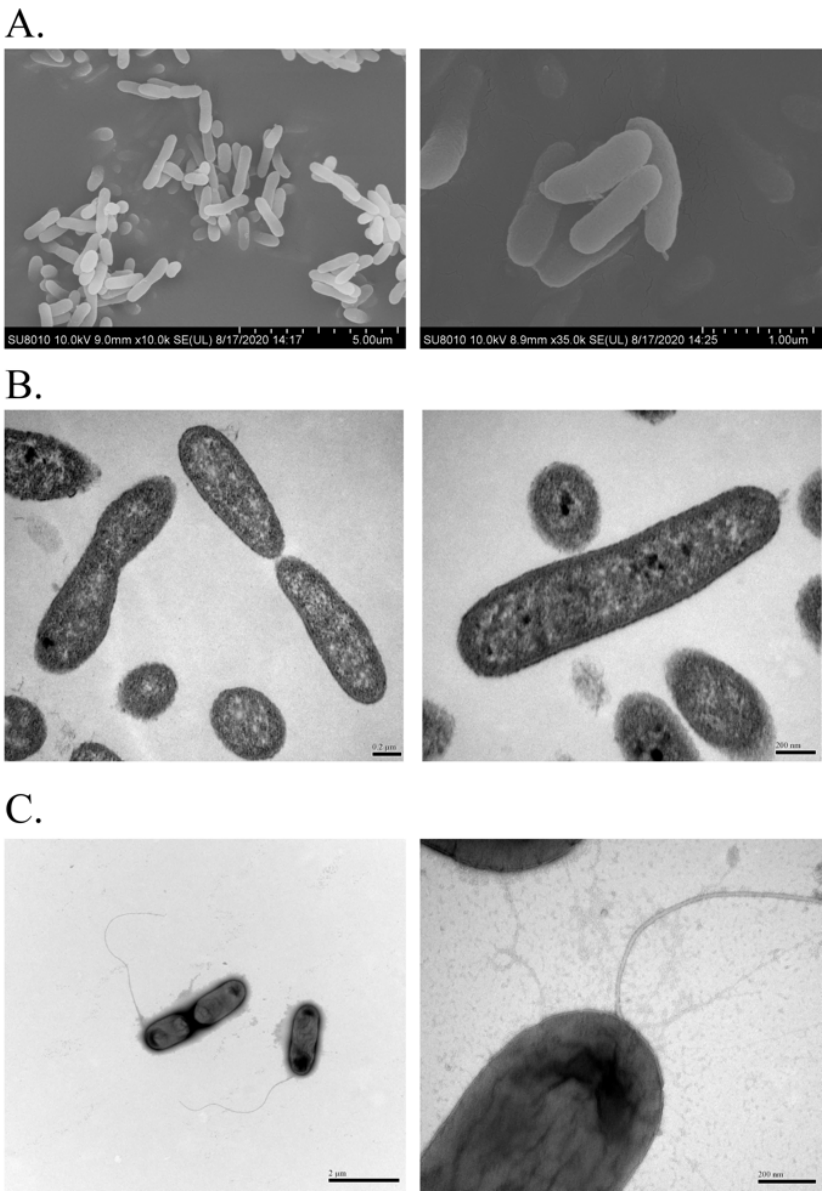


**Figure 1**

Cell morphology of strain SCS 2-3. (A) Scanning electron microscope (SEM) images; (B) Transmission electron microscopy (TEM) images; (C) TEM image of negatively stained cell showing flagella.

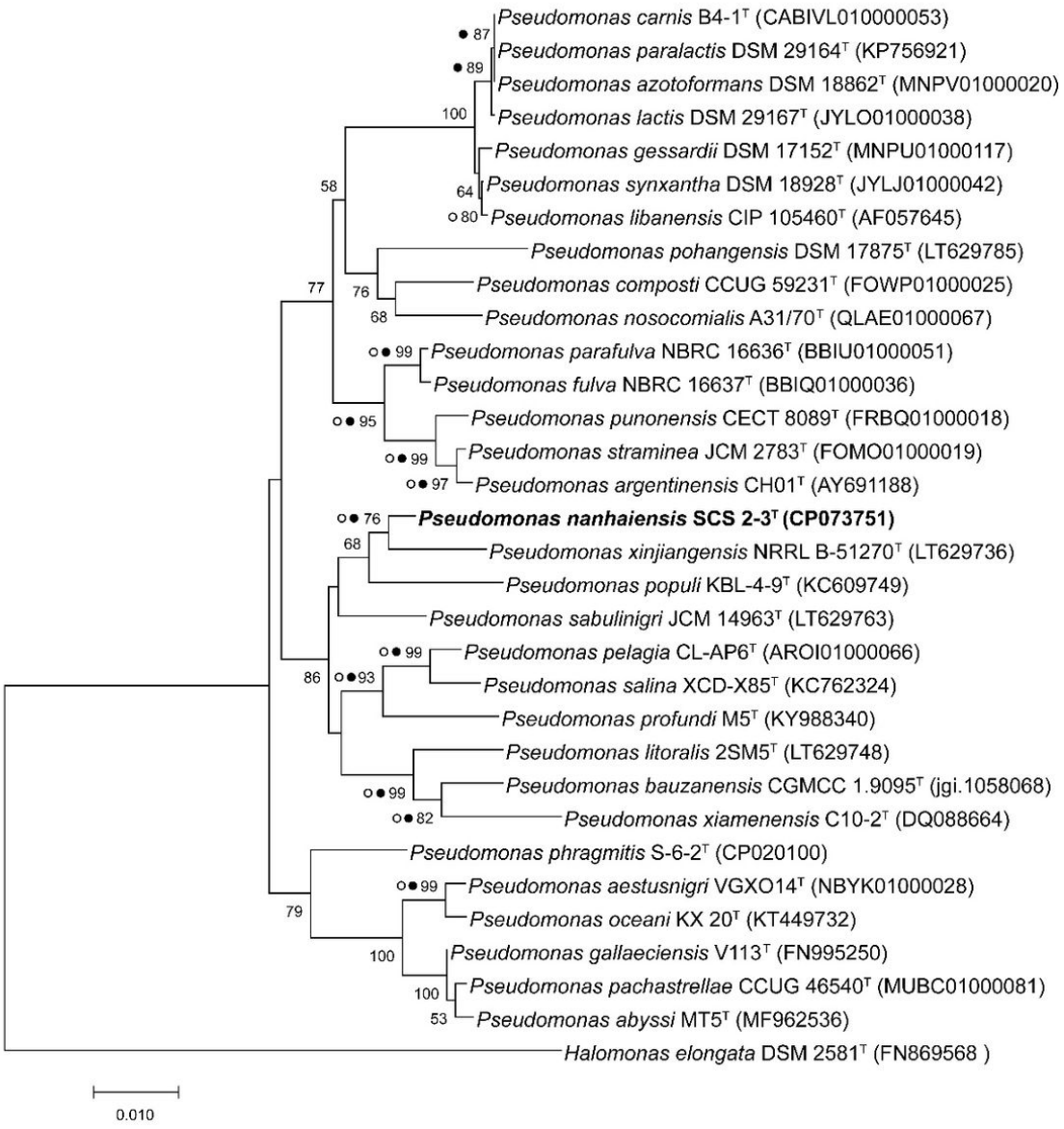


## Figure 2

Phylogenetic tree based on the 16S rRNA gene sequences using neighbor-joining (NJ) algorithm. The tree was rooted using Halomonas elongata DSM 2581T as the outgroup. Bootstrap values (> T50%) are shown at the nodes. Open circles (○) represent branches recovered in maximum likelihood (ML) tree and closed circles (●) represent branches recovered in maximun parsimony (MP) tree.

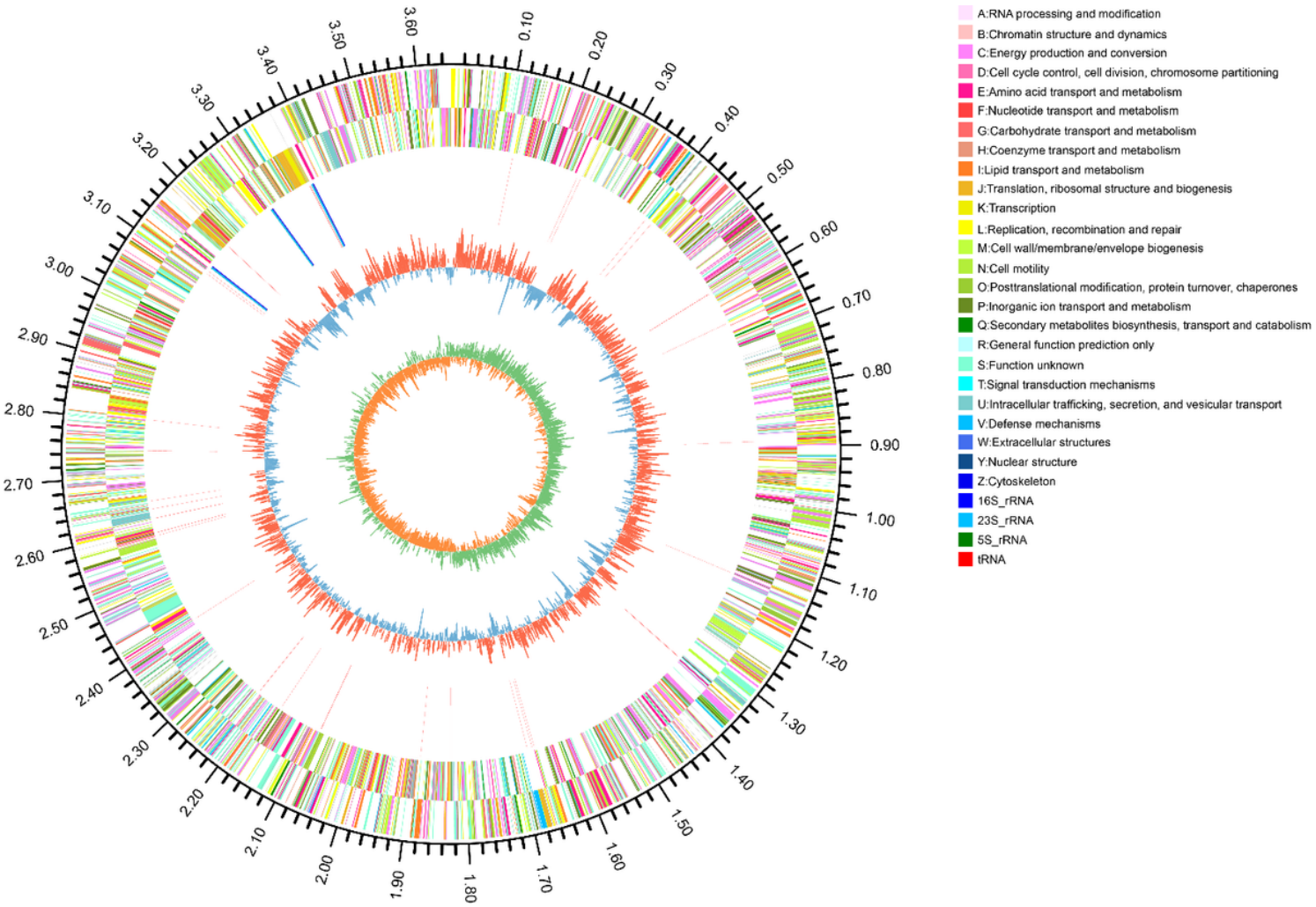


## Figure 3

The whole genome sequences of strain SCS 2-3. The genome map is composed of seven circles. From outside to inside, each circle displays information regarding the genome of (1) forward CDS, (2) reverse CDS, (3) forward COG function classification, (4) reverse COG function classification, (5) nomenclature and locations of predictive secondary metabolite clusters, (6) G+C content and (7) GC skew.

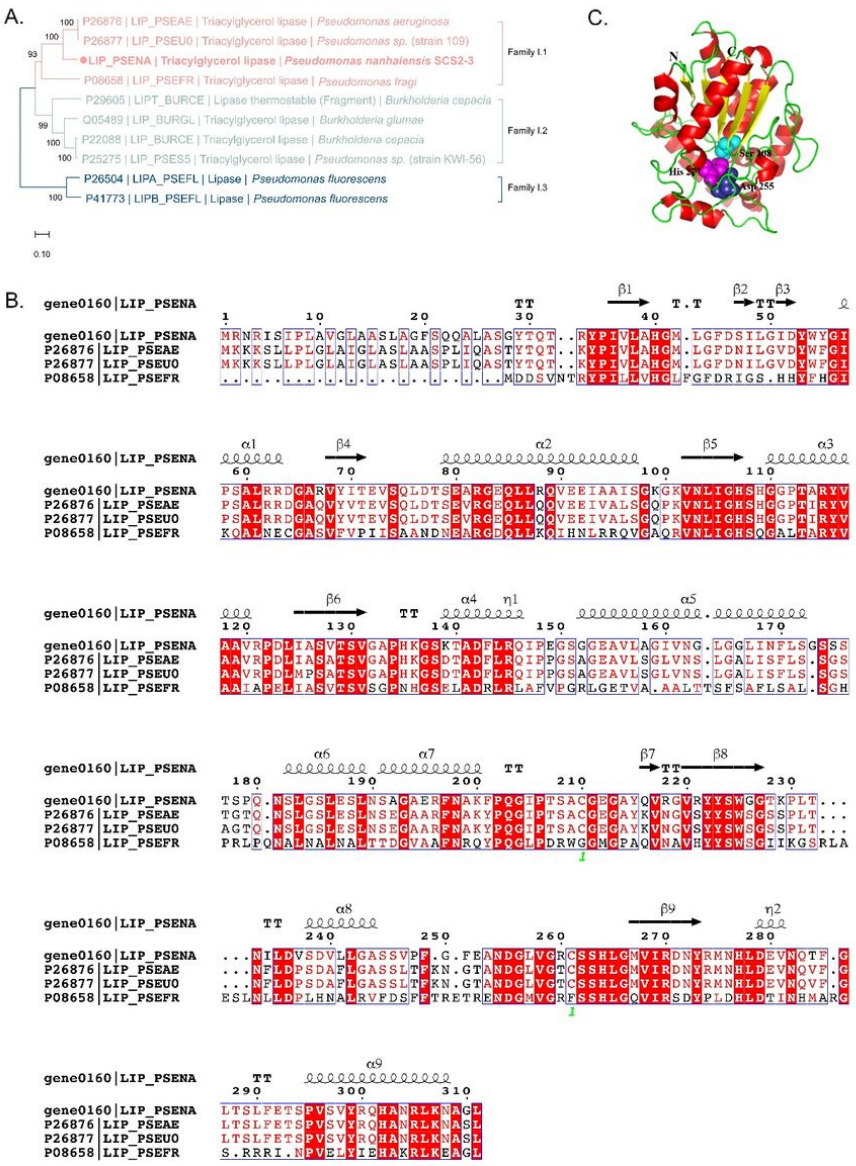


**Figure 4**

Lipase sequence analysis for strain SCS 2-3. (A) Phylogenetic tree of Lipase and other related lipolytic enzymes reviewed in UniprotKB database. The phylogenetic analysis was constructed with the neighbor-joining method of MEGA X. The values at nodes indicated the bootstrap percentage of 1,000 replicates, the lengths of the branches shown the relative divergence among the reference lipase amino acid sequences, and the scale bar indicated the amino acid substitutions per position. (B) Multiple sequence alignment between the lipase (gene0160) of SCS 2-3 and other family I.1 lipases. ClustalW2 and ESpript 3.1 were used to analyze multiple sequence alignment. The alpha helix, beta sheet, random coil, and beta turn are identical to α, β, η and T, respectively. (C) 3D model of Lipase. The α-helix, β-sheet and random coil are shown in the cartoon in red, yellow and green, respectively. The catalytic triads (Ser108, Asp255 and His277) are shown as spheres in cyan, blue and magenta, respectively. “N” and “C” denote the N and C termini, respectively.

## Supplementary Files

This is a list of supplementary files associated with this preprint. Click to download.

- SCS23supplementarymaterial5.12.docx